

Comprehensive Study on Seismic Subsidence of Loess under Earthquake

ZHANG Zhen-zhong¹, ZHANG Dong-li^{1,2}, LIU Hong-mei¹

(1. Lanzhou Base of Institute of Earthquake Prediction, CEA, Lanzhou, 730000, China;
2. Institute of Engineering Mechanics, CEA, Harbin, 150080, China)

Abstract: In this paper, the forming conditions of seismic subsidence of loess, the characteristics of seismic disaster, the basic properties of loess including water collapsibility relating to 1995 Yongdeng M_s 5.8 earthquake are discussed. The relationship between the static and dynamic parameters of loess and its seismic subsidence is also revealed. Using calculating method of predicting amount of seismic subsidence and 3D finite element method, proposed theory and method of seismic subsidence is validated and the seismic subsidence in 1995 Yondeng 5.8 earthquake is explained.

Key words: Seismic subsidence of loess; Disaster; Numerical analysis; Validating

黄土震陷灾害典型震例的综合研究

张振中¹, 张冬丽^{1,2}, 刘红玫¹

(1. 中国地震局地震预测研究所兰州基地, 甘肃兰州 730000;
2. 中国地震局工程力学研究所, 黑龙江哈尔滨 150080)

摘要: 阐述了1995年甘肃永登5.8级地震时造成的黄土震陷灾害形成条件、震害形态特征、黄土的基本性质及湿陷性和静、动土力学参数与震陷灾害的成因关系。并用震陷量预测计算方法和三维有限元数值模拟方法检验了黄土震陷灾害预测的理论、方法并解释了永登5.8级地震黄土震陷现象。

关键词: 黄土震陷; 灾害; 数值分析; 验证

中图分类号: P315.9 文献标识码: A 文章编号: 1000-0844(2005)01-0036-06

0 Introduction

On July 22, 1995, M_s 5.8 earthquake occurred in Qishan Village of Yongdeng county, Gansu Province of China. The epicenter locats at 103°E , 36.5°N with focus depth of about 10 km. The intensity of meizoseismal area is VIII. The total area of with intensity VII and VIII is 278 km^2 (Fig. 1). In the earthquake, 10 peoples were killed, 143 people were injured grievously and 584 were injured slightly. More than twenty thousand houses, 24 km road and 16.5km irrigation trench were de-

stroyed. The direct economy loss is up to a hundred million Chinese Yuan.

The seismic area is located at the western margin of Longxi Basin in loess plateau, where the geomorphologic units are mainly loess Liang (Chinese word for loess ridges) and Mao (Chinese word for round shaped loess hills). Malan loess of Late Pleistocene epoch (Q_3) with maximum depth of 40 m and Lishi loess of Mid Pleistocene epoch (Q_4) are distributed widely. The underlying bedrock is

收稿日期: 2004-06-14

基金项目: 国家自然科学基金项目(50379049); 中国地震局兰州地震研究所论著编号: LC2004033.

作者简介: 张振中(1936-), 男(汉族), 上海崇明人, 研究员, 主要从事黄土动力特性及黄土地震灾害预测与预防研究。

sandstone of Tertiary and Cretaceous System.

After earthquake, many scholars in fields of seismology, geology disaster and engineering circle including the first author of this paper studied and presented views from different aspects based on field investigation, measurement, laboratory test and theory analysis and a number of papers were published. The authors think that this is a typical disaster of loess seismic subsidence since the concept of loess seismic subsidence was put forward. Therefore, it must be useful to make a comprehensive report based on the integrated analysis using all the related materials and the research results [1].

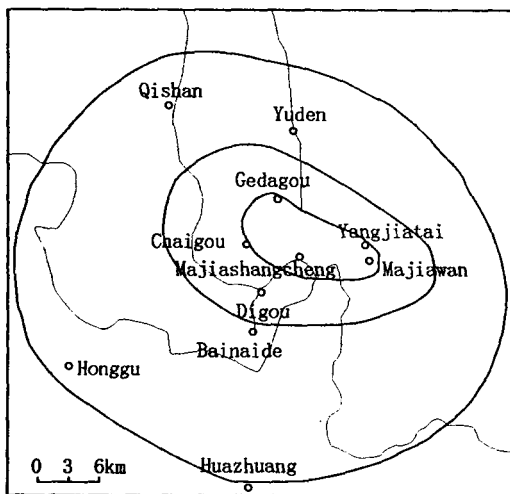


Fig. 1 The isoseismals of $M_s 5.8$ earthquake in Yongdeng, 1995.

1 Characteristic of Seismic Subsidence

Though the magnitude of Yongdeng earthquake is not very high, due to earthquake vulnerability of loess, landslides, serious seismic subsidences occurred. In the area of VII and VIII intensity, 150 landslides distributed, most of them are small-scale slides (30 m long and 40 m wide) in near surface soil layer (2~3 m deep).

Severe seismic subsidence occurred in loess. On the top of hill many tensile fissures and smashing damages developed (Fig. 2). The top of Liang is relatively flat and at the flank of Liang the surface shows inclination of $2^\circ \sim 3^\circ$, then transits to loess slope. Generally, the slope angle is

around $25^\circ \sim 45^\circ$. Although there are many fissures on the top of Liang, the lower part of Liang remained almost untouched and neither obvious deformation nor slides were found after the earthquake. The fissures at the two sides of Liang incline towards the middle and form ladder-like dislocations revealing the inhomogeneous seismic subsidence. At the middle, there shows the signs of smashing damage and the seismic subsidence stands at 30 to 40 cm most, the maximum amount reaches 52 cm (Fig. 3 to Fig. 4). Later the mechanism of this kind of seismic subsidence will be explained through numerical analysis.

2 Formative Condition of Seismic Subsidence

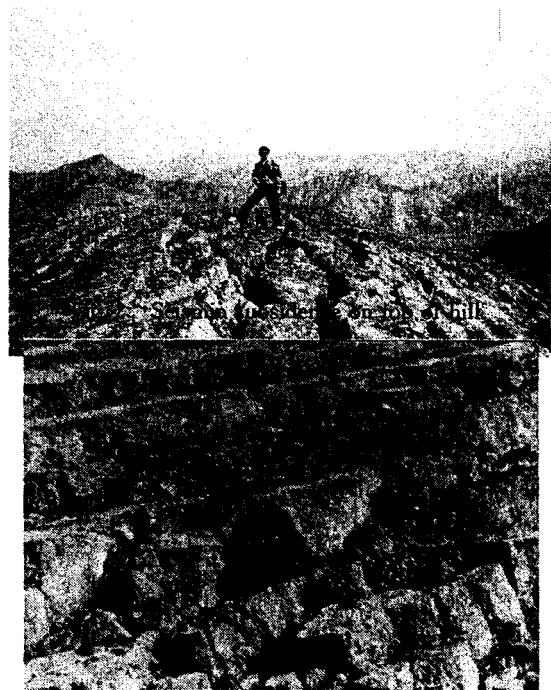


Fig. 3 Ladder-like dislocations.



Fig. 4 Fissure of seismic subsidence on one side of hill peak.

2.1 Basic Property of Loess

The thickness of Malan loess of Late Pleistocene in the earthquake affected area is around 25~30 m. It is a kind of light yellow, loose and dry loess with eye identifiable wormholes, big pores, plant roots and white calcareous mycelium. Vertical joints well developed under natural conditions. Physical indices obtained from tests on samples from Gadagou, Majiashancheng, Chaigou and Yangjiatai in meizosismal area listed in Table 1. Table 2 gives the criteria for discriminating proper-

ty of seismic subsidence of loess.

What is need to be mentioned is that heavy rain both before and after earthquake increased the water content of loess layer to be fairly high, but during the time samples were secured from the sites almost one year after the earthquake the water content in samples was much lower and mostly around the shrink limit of loess. The loess sample has void ratio of is around 1.2 and with high water collapsibility and self-weight water collapsibility. They are very porous indeed.

Table 1 The Physics Parameters of Loess in Yongdeng Earthquake Area

Soil sample numbers	Depth/m	$\gamma/[\text{kN} \cdot \text{m}^{-3}]$	$\gamma_d/[\text{kN} \cdot \text{m}^{-3}]$	$w/\%$	G_s	e	Gradation/%		
							Sand	Silt	Clay
Y1	4.0	12.35	11.86	4.53	2.70	1.231	10.1	72.6	17.3
Y2	4.0	12.35	11.96	4.31	2.70	1.231	19.8	63.8	16.4
Y3	4.0	12.35	12.05	5.21	2.70	1.195	19.0	66.3	14.7
Y4	4.0						18.1	63.4	18.5

Table 2 The Criterion of Seismic Subsidence

Sample No.	w	e	w_L	w_P	I_P	W_s	200 kPa δ_s	δ_{s*}
Y1	4.53	1.231	27.2	18.3	8.9			
Y2	4.31	1.231	25.5	17.3	8.2	4.4	19.43	16.1
Y3	5.21	1.195	28.1	19.8	8.3	5.2	17.51	10.5
Y4			24.6	15.6	9.0	4.6		

Besides physical indices, scanning electronic microscope (SEM) analysis of microstructure of loess has been done. The purpose is to seek relationship between dynamic parameters and characteristics of loess microstructure. But the quantification can be done at this stage provides only the size of pores and their area distribution, instead of a concrete value which cannot be realized now^[2]. Despite of that, the analysis on characteristics of microstructure and quantification of pore composition is still a better way to study the mechanism of loess seismic subsidence. Malan loess formed in later Pleistocene has trellis structure pores with grain contact. This kind of large pores control the seismic subsidence of loess^[3]. The large pores accounts for 92.09% of all area of pores and with maximum radius of 202 μm . In the undisturbed samples secured from sites affected by the earthquake, it is found that some of the trellis structure pores were partially damaged and changed into plane contact mosaic-like pores. Thus trellis structure pores collapse to become inter-particle

pores and subsequently, the area of trellis structure pores were reduced to only 13.14% of area of all pores in loess sample affected by the earthquake. This phenomenon reflects the mechanism of seismic subsidence of loess (Fig 5, 6).

2.2 Soil Dynamic Parameters

From table 3, it is shown that the initial elastic modulus of loess is very low. Combined with the physical indices in Table 3, it shows that the loess in Yongdeng has rather loose structure and weak seismic resistance.

2.3 Coefficient of Seismic Subsidence

Seismic subsidence tests result on loess samples secured from Yongdeng earthquake affected sites is shown in Fig. 7. The result shows that the seismic subsidence or residual strain of loess increases with the growth of dynamic stress but with great variation for different loess samples is also indicated. Under dynamic stress of 100 kPa, residual strain of three groups of loess samples ranges 0.78%~2.75%. Also, larger residual strain developed if the water content is higher.

Table 3 Dynamic Parameters of Loess in Yongdeng Earthquake Area

Sample No.	w/%	e/kPa	σ_{1c} /kPa	σ_{3c} /kPa	Measurement times	E_{dmax} /MPa	$a/10^{-3}$	b	Correlation coefficient	Damping ratio
Y1	4.84	1.250	50.8	30.0	11	51.33	1.948	1.3874	0.996	0.120~0.138
Y2	3.78	1.231	50.8	30.0	10	67.83	1.474	0.7817	0.984	0.110~0.124
Y3	5.03	1.160	52.4	30.9	8	69.58	1.437	1.1492	0.994	0.102~0.120

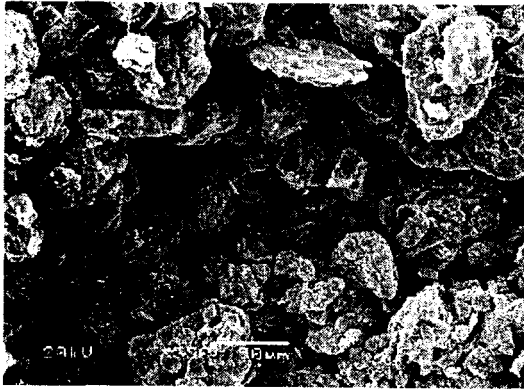


Fig. 5 Trellis structure pore in sample Yong-2.

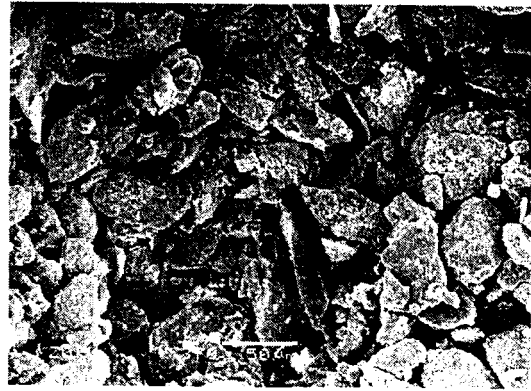


Fig. 6 Mosaic structure pores form due to collapse of trellis structure pores in sample Yong-2 .

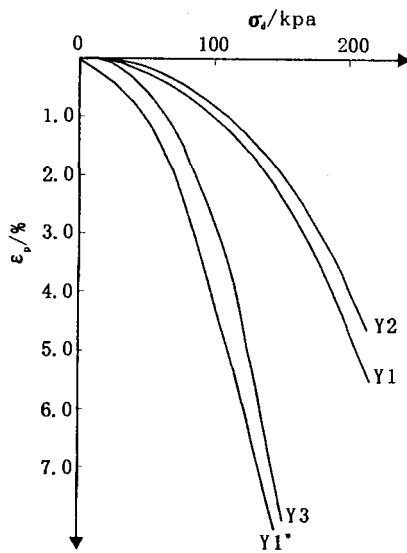


Fig. 7 Test result of seismic subsidence of Yongdeng loess.

Generally, when the water content of loess is lower than 10% or in another way, near shrink limit, the loess is rather strong and is called dry loess, which will not develop obvious residual strain under earthquake intensity of VIII. But the sediment and palaeoclimate condition made the loess in some part very loose and almost without cementation. Consequently, the water content of Y3 is around 5% but residual strain still developed much.

In order to simulate high water content condi-

tion, sample Y1 was wetted to raise its water content from 4.53% to 12%. As a result, the coefficient of seismic subsidence increases rapidly and the critical dynamic stress is nearly zero. The initial pressure of collapse of Y2 and Y3 are 2.0 kPa and 3.2 kPa respectively, which is approximately amount to their initial stress of seismic subsidence. This proves that there are similarities between seismic subsidence and water collapse of loess as proposed by the first author earlier. Under the dynamic stress of 100 kPa, the residual strain increases from 1.0% to 4.15% for the wetted sample Y1, this means that the water content is a major factor influencing the seismic subsidence of loess.

The above-mentioned analysis shows that the study results are confirmed by earthquake investigation and validated the study on macro earthquake disaster phenomenon. At the same time, it proves that the method on seismic subsidence coefficient calculation get reliable results compared with real loess seismic subsidence.

2.4 Estimation on seismic subsidence of loess and its validation

Using the estimation method of seismic subsidence, amount of seismic subsidence in Yongdeng earthquake affected area under intensities of VII, VIII and IX are calculated (Table 4).

Table 4 Check Results of Seismic Subsidence of Loess Sites in Yongdeng

Sites	Sample number	Depth of calculation /m	Maximum seismic subsidence /cm		
			Ⅵ	Ⅶ	Ⅷ
Chaigou	Y1	20	1.1	4.9	20.8
	Y1* (wetted)	20	9.2	26.8	101.7
Majiashancheng	Y2	20	0.7	3.3	17.3
Gadagou	Y3	20	2.7	11.7	63.9

From table 4, it shows that the amount of seismic subsidence increases with the increase of seismic intensity. Under intensity Ⅵ, there is only slight seismic subsidence while under intensity Ⅷ there is severe seismic subsidence with average amount of around 30 cm. Particularly, the amount of seismic subsidence of wetted sample Y1* reaches as large as 26.8 cm under seismic intensity Ⅶ compared with that of 4.9 cm of samples secured from the same location without wetting. Then, it can be concluded that raining increased water content and subsequently caused severe seismic subsidence in the seismic area. Compared with the water collapsibility criterion of loess, once again, it is found that loess with high water collapsibility often develops large seismic subsidence under certain earthquake effect.

3 Numerical Analysis on Seismic Subsidence

3.1 Method

Using 3D FEM procedure, calculation on seismic subsidence at North Liang of in Gadagou village, in Yongdeng earthquake meizoseismal area is carried out.

The 3D calculation is done with the simplified model, which uses cross section with equal distance along the strike of the Liang to calculate the 2D seismic subsidence and then combine all the information together to indicate the 3D seismic subsidence. This procedure is actually a pseudo-3D approach. The input waves are respectively with exceedance probabilities of 63.5%, 10% and 2% in 50 years.

3.2 Results of Seismic Subsidence Calculation

Under earthquake loading, the permanent deformations are very large both in horizontal and

vertical directions. Under the ground motion with exceedance probability of 2% in 50 years (equivalent 8.6 in seismic intensity), the maximum seismic subsidence occurs on the top of Liang which ranges from 15 cm to 50 cm. Demarcated at the middle line along the strike direction on the top of Liang, the horizontal deformations develops at opposite direction at the opposite side of the Liang. At Gadagou, in the meizoseismal area the simulation seismic intensity is from 7.8 to 8.6, which conform to the actual seismic intensity Ⅶ. The seismic subsidence calculated ranges from 27.2 cm to 51.3 cm, which tallies well with the actual measurements on seismic subsidence (Fig. 8).

3.3 Mechanism of Seismic Subsidence

The numerical analysis results explain the ladder-like dislocations of 30~40 cm on relatively level top of the Liang and the tensile fissures. Fig. 8 shows that the maximum settlement is at the middle of the top. Under the seismic loads both at vertical and horizontal directions, deformation with vertical/horizontal ratio from 1.4:1 to 3:1 develops. The vertical deformation causes the settlement and horizontal deformations push the loess at the opposite side from the middle of Liang to move apart. Since the vertical deformation is larger than horizontal deformation, the ladder-like dislocation inclines towards the top of the Liang, which also reflects the fact that loess layer, formed graben-like dislocation towards the center of settlement (Fig. 9). This phenomenon can be substantially differentiated from landslide^[4].

4 Conclusion

Loess earthquake disaster in Yongdeng has given examination to the theories, testing and analyzing techniques and predicting methods of loess seismic subsidence from all aspects.

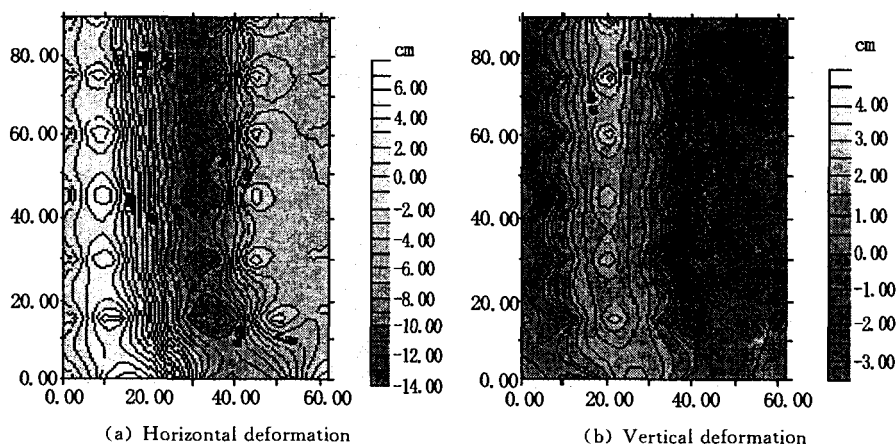


Fig. 8 Contour chart of deformation of loess hill.

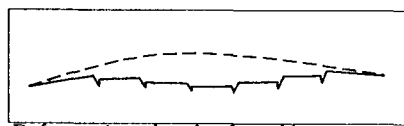


Fig. 9 Deformation sketch of profile on top of Liang.

(1) The causal conditions of loess seismic subsidence are described based on the basic properties of loess, which can be used to evaluate the seismic subsidence of loess. The first author found that self-weight water collapsible loess with water content higher than shrink limit and void ratio more than 0.8 usually could develop seismic subsidence under strong ground motion. The wetted sample Y1[#], whose water content was increased to 12% from 4.53%, produced residual strain of 4.15% compared with that of 1.0% of undisturbed sample Y1. This shows that water content has a clear effect on seismic subsidence of loess. Since loess in Yongdeng seismic area has void ratio of around 1.2 and is with high self-weight water collapsibility, naturally, it could develop large seismic subsidence during earthquake. The maximum amount of seismic subsidence is as large as 50 cm, which can be classified as severe seismic subsidence, in seismic area in Yongdeng. There are certain similarities between water collapsibility and seismic subsidence of loess. In this study, the initial stress of water collapsibility is as low as 2 to 3 kPa and critical stress of seismic subsidence corresponding are also at similar value.

(2) All the loess with trellis structure pores can occur seismic subsidence under certain earthquake condition. The analysis on the SEM images

of microstructure of loess can not only evaluate the seismic subsidence of loess but also provide evidence to explain the mechanism of seismic subsidence of loess. The samples secured from the seismic area are all with trellis structure pores, which is subjected to smashing damage and seismic subsidence developed. Importantly, the partial damage of trellis structure pores was observed from the undisturbed sample secured from seismic area. It proves that trellis structure pores can be changed into mosaic pores so this kind of large pores become inter-particle pores. Taking sample Y2 as example, the area of large pores in sample secured after the earthquake decreased to 13.14% of area of all pores calculated from that of 92.09% in samples unaffected by the earthquake. This could be regarded as the direct evidence that the seismic subsidence of loess is caused by the collapse of trellis structure pores existing in loess.

(3) The methods of calculating and predicting seismic subsidence of loess are examined. Both conventional and numerical methods of estimating seismic subsidence of loess go well with the actual seismic subsidence measured in situ. The seismic subsidence in meizoseismic area is around 30 cm mostly, but the maximum amount of seismic subsidence is as large as 50 cm. Using the ratio of vertical to horizontal deformation got from numerical analysis the ladder-like dislocation at the two sides of Liang were explained as results of seismic subsidence instead of landslide.

3.3 随机模型的确定

通过对6个回归方程的 F 值和回归变量的 T 值的综合分析比较后认为,四模型参数 I_0 、 c 、 t_1 及 $t_s = t_2 - t_1$ 随 x 向和 y 向测点坐标及土层厚度 h 的变化的随机模型为

$$\begin{aligned} I_0 &= a \cdot x + b \cdot y + c \cdot h^{1.5} + d; \\ c &= a \cdot x + b \cdot y + c \cdot h^{1.5} + d; \\ t_1 &= a \cdot x + b \cdot y + c \cdot h + d; \\ t_s &= a \cdot x + b \cdot y + c \cdot h + d. \end{aligned} \quad (2)$$

即四模型参数与随 x 、 y 向测点坐标及土层厚度 h 的变化而变化。

从表4中回归系数的正负号来看, I_0 、 c 和 t_1 均随 x 向距离和土层厚度 h 的增大而减小; t_s 则随着随 x 向距离和土层厚度 h 的增大而加长。 y 向距离在各次地震中对各参数的影响不一致,从总体来看, I_0 、 c 随 y 向距离的增加而增加; t_1 和 t_s 随 y 向距离的增加而减小。

3.4 理论预测模型

在多点地震动时程合成中,利用 i 点的参数值 I_{0i} 、 c_i 、 t_{1i} 和 t_{si} ,及 i 、 j 点间的距离 Δx 、 Δy 和土层的厚度差 Δh ,按以下模型来推算 j 点的参数值:

$$\begin{aligned} I_{0j} &= I_{0i} + a \Delta x + b \Delta y + c \Delta h^{1.5}; \\ c_j &= c_i + a \Delta x + b \Delta y + c \Delta h^{1.5}; \\ t_{1j} &= t_{1i} + a \Delta x + b \Delta y + c \Delta h; \\ t_{sj} &= t_{si} + a \Delta x + b \Delta y + c \Delta h. \end{aligned} \quad (4)$$

4 结论

通过对SMART-1三次地震各测点竖向地震记录的统计回归分析得出以下结论:

(1) 在三种拟合条件下,拟合条件B的收敛性

最好,条件A次之,条件C则稍差。对于不同地震不同测点,竖向强度包络模型中四模型参数的取值各不相同,即使是同一次地震的同一记录,因拟合条件的不同,参数的取值也不完全相同。

(2) 竖向地震动时程中三阶段——上升段、平稳段和衰减段的能量占总能量的百分比接近于10%、70%、20%。

(3) 竖向强度包络模型中四模型参数(I_0 、 c 、 t_1 和 $t_s = t_2 - t_1$)的大小随二维空间距离和土层厚度的变化而变化,变化规律如公式(2)表示。

从模型的回归系数的正负号来判断, I_0 、 c 、 t_1 随 x 、 h 的增加而减小, t_s 随 x 、 h 的增加而增加; I_0 、 c 随 y 的增加而增加, t_1 、 t_s 随 y 的增加而减小。

(4) 由 i 点参数值推算 j 点参数值的模型如公式(4)所示。

[参考文献]

- [1] 屈铁军. 地面运动的空间变化特性研究及地下管线地震反应分析[D]. 哈尔滨: 国家地震局工程力学研究所, 1995. 16-37.
- [2] 程岩. 竖向地震作用对高柔结构的影响[J]. 西北地震学报, 1999, 21(4): 423-427.
- [3] 大崎顺彦著. 吕敏申, 谢礼力译. 地震动谱分析入门[M]. 北京: 地震出版社, 1980. 168-171.
- [4] Amin M, Ang A H - S. Nonstation Stochastic Model of Earthquake Motion[J]. J. EM. ASCE. , 1968, 94(2): 559-583.
- [5] H Takizawa, P C Jennings. Collapse of a Model for Ductile Reinforced Concrete Frames Under Extreme Earthquake Motions[J]. EESD, 1980, 8(2): 117-144.
- [6] 朱勇华, 邵淑彩, 孙福玉. 应用数理统计[M]. 武汉: 武汉水利电力大学出版社, 1999. 188-194.

(上接41页)

[References]

- [1] Zhang Z Z. Prediction of Seismic disaster in Loess area[M]. Beijing: Earthquake Press, 1999.
- [2] Xie D Y, Zhang J M, et al.. Constitutive relation considering the structure of soil[J]. Journal of civil engineering, 2000, 33(4): 36-41.
- [3] Qi J L. Pore distribution curves of loess structure porosity by quantitative analysis[J]. Northwest Seismological Journal, 1997, 19 (supplement): 83-87.
- [4] Zhang D L, Wang L M. The computer-added analogue and the mechanics analysis about mountain ground deformation induced by Yongdeng earthquake in 1995[J]. Northwest Seismological Journal, 2003, 25 (1): 77-81.